Available online at www.sciencedirect.com

ScienceDirect

journal homepage: www.elsevier.com/locate/he

A DFT study on the hydrogen desorption from the lithium borohydride and aluminohydride upon the addition of nanostructured carbon catalyzing agent

C. Paduani[*], *Andrew M. Rappe*

The Makineni Theoretical Laboratories, Department of Chemistry, University of Pennsylvania, 231 S. 34th Street, Philadelphia, PA 19104-6323, USA

ARTICLE INFO

Article history:
Received 1 August 2016
Received in revised form
15 September 2016
Accepted 18 September 2016
Available online 13 October 2016

Keywords:
DFT
Light metal hydrides
Dehydrogenation
Catalyst

ABSTRACT

Here we study in van der Waals-corrected DFT calculations the dehydrogenation mechanism of the light metal hydrides $LiBH_4$ and $LiAlH_4$ by focusing on the effect of the addition of the carbon fullerene C_{60} as catalyzing agent. The results show a rather significant gain in the energy cost for H desorption in the presence of the catalyst, which is substantially even more pronounced when considering boron-doping the fullerene. In the source of this effect is the disturb introduced in the distribution of bonding charge upon the hybridization of states in the interplay cluster-fullerene with a consequent weakening of the hydrogen bonds, leading therein to an enhanced kinetics for the hydrogen release.

Introduction

With the urge for producing clean energy, since we have far more oil that we can safely burn, hydrogen, as a energy carrier, is nowadays considered as one of the best alternatives for mobile and stationary power sources for both propulsion and fuel cells. One of the major drawbacks of this technology is however the problem of storing hydrogen safely, since in both liquid and gas form this demands high pressure or cryogenic reservoirs. A promising solution could be the use of solid state hydrogen storage. Among the materials which are good candidates for this purpose are the complex light metal hydrides [1–15], where the hydrogen atoms are held by strong covalent bonds. Particularly attractive is $LiBH_4$, which has a high volumetric hydrogen density (18.5 wt%) [16]. However, being highly stable, high temperatures are required for the hydrogen desorption. As an attempt to surpass this difficulty the addition of catalysts has been considered, and among them, Ti has indeed proven to be a feasible option to facilitate the release of molecular hydrogen at low temperatures [17,18].

The addition of catalysts to complex hydrides is aimed to enhance the hydrogen sorption properties. Studies on the use of carbon nanomaterials as catalysts in conjunction with complex metal hydrides showed remarkable properties [19–21]. For instance, the buckminsterfullerene C_{60} has proved to be an excellent catalyst for hydrogen desorption when added to $Mg(BH_4)_2$, $NaAlH_4$, $LiAlH_4$ and $LiBH_4$ [22–24]. A fullerene-$LiBH_4$ composite demonstrates remarkable catalytic

* *Corresponding author*. DF-UFSC, Florianópolis CEP 88040-900, SC, Brazil. Fax: +55 48 3721 9946.
E-mail address: clederson.paduani@ufsc.br (C. Paduani).

http://dx.doi.org/10.1016/j.ijhydene.2016.09.124

effect [25]. Besides enhancing both the uptake and release of hydrogen, it provides lower hydrogen desorption temperatures as well as regenerative rehydrogenation at a relatively low temperature (350°C) in addition to a reversible hydrogen capacity of 4.0 wt % over multiple cycles [23]. At higher fullerene contents, in composites comprised of C_{60} with $NaAlH_4$ and $LiAlH_4$, hydrogen is desorbed at lower temperatures. The resultant alkali metal fulleride containing composites were found to be capable of reversible hydrogen storage. This catalytic effect has been discussed as probably originating from C_{60} interfering with the charge transfer from Li to the BH_4 complex, resulting thereof in weaker B–H bonds. Experimental results of laser vaporization of a graphite pellet containing boron nitride powder was found to produce fullerenes in which one or more atoms of the hollow carbon cage was replaced by a boron atom [26].

In this work we investigate the hydrogen desorption from the light metal hydrides $LiBH_4$ and $LiAlH_4$ by considering the effect of the use of a nanostructured carbon catalyst, i.e., the buckminsterfullerene C_{60}. Besides a comparison between the performance of the lithium borane and alanate in this reaction, in this study we focus also on the effect of boron-doping the fullerene, and therein following the consequent changes in the equilibrium geometries, charge distribution, binding energy and energy cost for hydrogen desorption. The results show that upon boron-doping the catalysing agent the one-electron deficiency disturbs the local symmetry in the adduct complexes and affects the coordination centre of the metal hydrides in such a way that results in weaker intracluster interactions, thereby contributing to ease the dehydrogenation process. This study provides new insight in the understanding of the hydrogen sorption mechanism of the light metal hydrides.

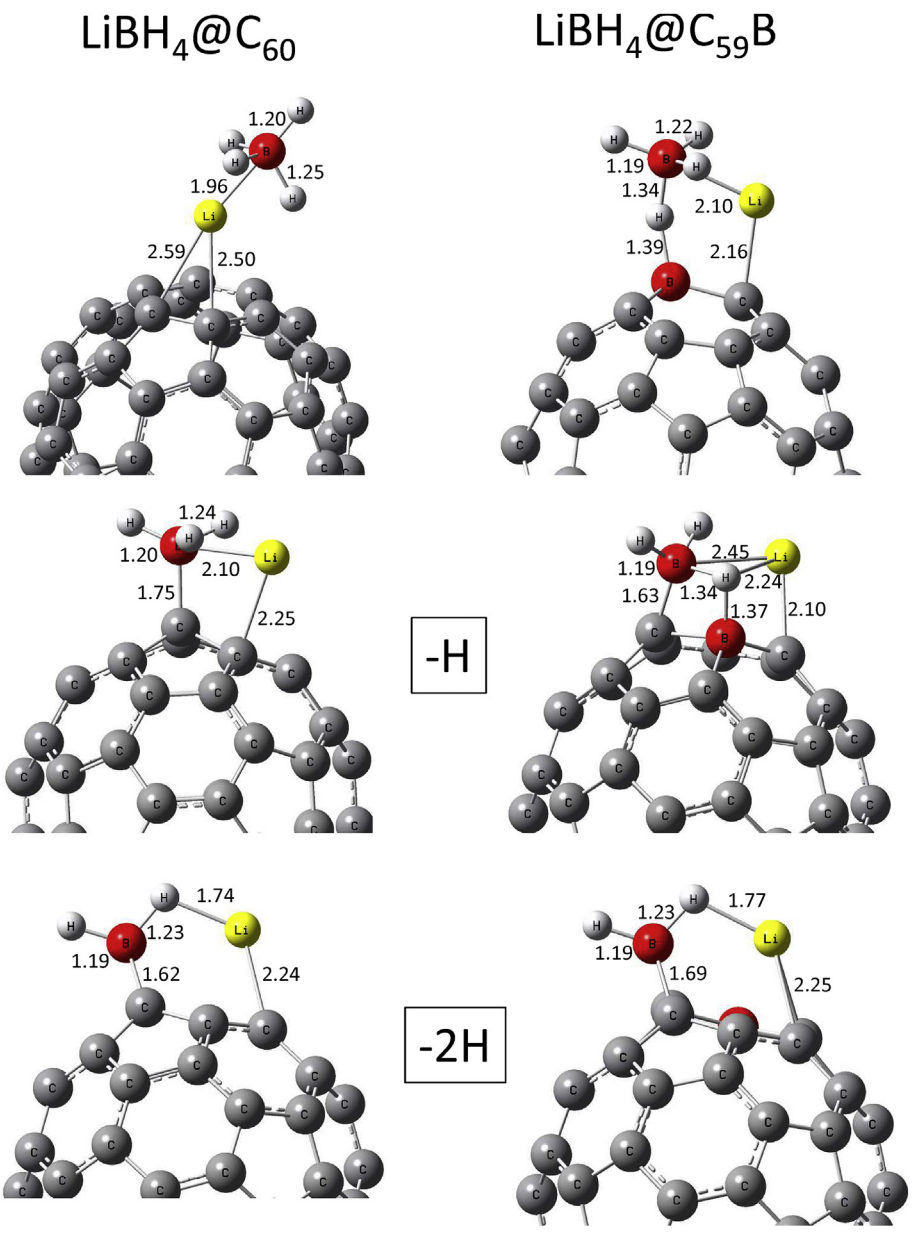

Fig. 1 – Optimized geometries for $LiBH_4$ supported on both pristine and B-doped C_{60} as one and two H atoms are removed (bond lengths (Å) are indicated).

Method

The vdW-DFT calculations are based on the density functional theory as implemented in the Quantum Espresso code [27]. For the pseudopotentials we adopted the Vanderbilt ultrasoft form with non-linear core corrections, generated by employing the Becke-Lee-Yang-Parr (BLYP) functional. For the treatment of the van der Waals dispersion interactions, which results from dynamical correlations between fluctuating charge distributions, we use the Grimme's DFT-D2 semi-empirical model [28–30], where the van der Waals interactions are described via a simple pair-wise force field [31]. For the geometry optimization the atoms were distributed in a simple cubic supercell with a lattice size of 25 Å, taken as large enough in order to prevent or minimize any interaction between the clusters. For the sampling in the Brillouin zone only the Γ point was considered in single point calculations. The plane wave cutoff was taken at 40 Ry, and the total energy was converged to 10^{-6} eV. All geometries were fully relaxed until the tolerance for interatomic forces were smaller than 0.001 eV/Å. In order to assure that the obtained equilibrium geometries are indeed the ground state structures, the relaxation process was performed with several different starting configurations.

Results and discussion

In Fig. 1 are shown the equilibrium geometries of the $LiBH_4$ cluster supported on the carbon fullerene C_{60} as the H atoms are successively removed. Near the C_{60}, the cluster stands at an upward orientation, where the Li atom is seen hovering close to a C–C bridge, distant of 2.50 Å from the nearest C atom. By removing one H atom, the $LiBH_3$ cluster (middle panel) assumes a sideway orientation, where the boron atom from the BH_3 complex is seen bonded to a C atom with bond length 1.75 Å. The fullerene is seen slightly distorted locally. The Li atom becomes farther away from the B atom (2.10 Å), and it is also seen bonded to a C atom (2.25 Å). Upon the next H removal the $LiBH_2$ cluster gets even closer to the fullerene, and the B atom is now seen tightly bonded to a C atom (1.62 Å). Interestingly enough is the fact that the Li atom still keeps the same distance from the fullerene (2.25 Å). Note how the C atoms are slightly pushed out of the structure of the fullerene in this reaction, whereas the B–H bond lengths remain practically unchanged.

On the right panels of Fig. 1 we show the same mechanism of H removal now by considering the doping of the fullerene with a boron atom replacing one C atom. In the top panel of Fig. 1 note the formation of a stronger Li–C bond (2.16 Å) and how one H atom binds strongly to the B impurity in the C_{59} B fullerene, with a B–H bond length of 1.39 Å, and therein resulting in an elongation of the B–H bond length (1.34 Å) within the ligand complex. Relatively to the pristine C_{60} we see now a local distortion in the doped buckyball. After the removal of one H atom, the $LiBH_3$ gets closer to C_{59} B, giving rise to the formation of stronger bonds: B–C (1.63 Å), B–H (1.37 Å) and C–Li (2.10 Å). Nevertheless, the fullerene is seen only slightly distorted. Upon the removal of the second H atom we see the $LiBH_2$ cluster going farther away from the cluster, with B–C and Li–C bond lengths of 2.36 and 2.25 Å, respectively. The remaining H atoms stand tightly bonded to the B atom of the ligand. The amount of energy necessary for removing $n(H)$ atoms from the $LiBH_4$ cluster is calculated as $\Delta E_n = E[Li(BH_4)] - E[LiBH_{4-n}] - E[n(H)]$, and the results are showed in the histograms of Fig. 2. The energy cost necessary for removing one H atom from the $LiAlH_4$ cluster decreases from 4.34 to 3.26 eV in the presence of C_{60}. For the doped C_{59} B system, this is even lower, i.e., 2.99 eV, thus characterizing a catalytic behavior for the fullerene. For the removal of the next H atom ΔE decreases from 4.99 to 3.54 eV, when adding the pristine C_{60}. With the boron-doping however, the energy cost increases to 4.08 eV, which is still lower than the result without the catalyst. This behavior arises from the fact that after the first H removal the $LiBH_3$ cluster becomes more strongly bonded to the doped fullerene, as pointed out above. The gain in energy for the first H removal when using the C_{60}

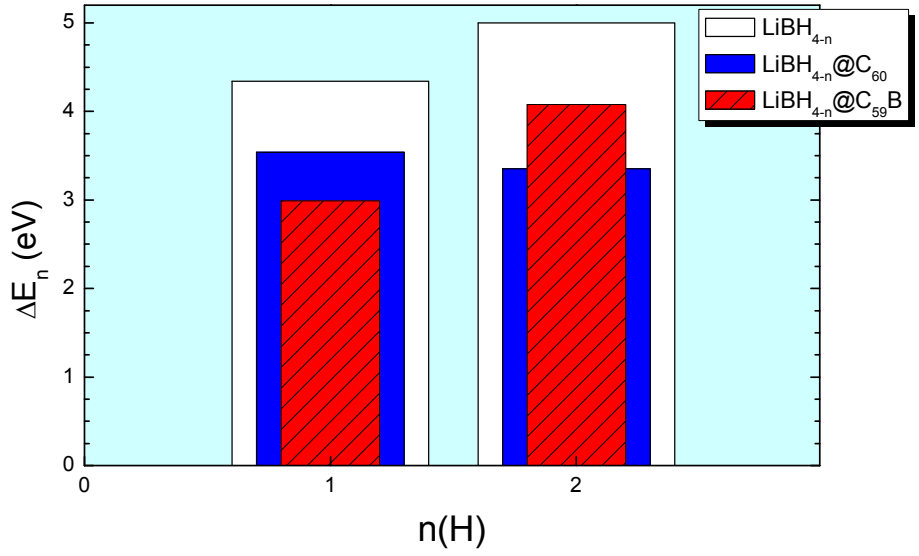

Fig. 2 – Energy cost Δ E (eV) for H-removal from $LiBH_4$, $LiBH_4@C_{60}$ and $LiBH_4@C_{59}B$.

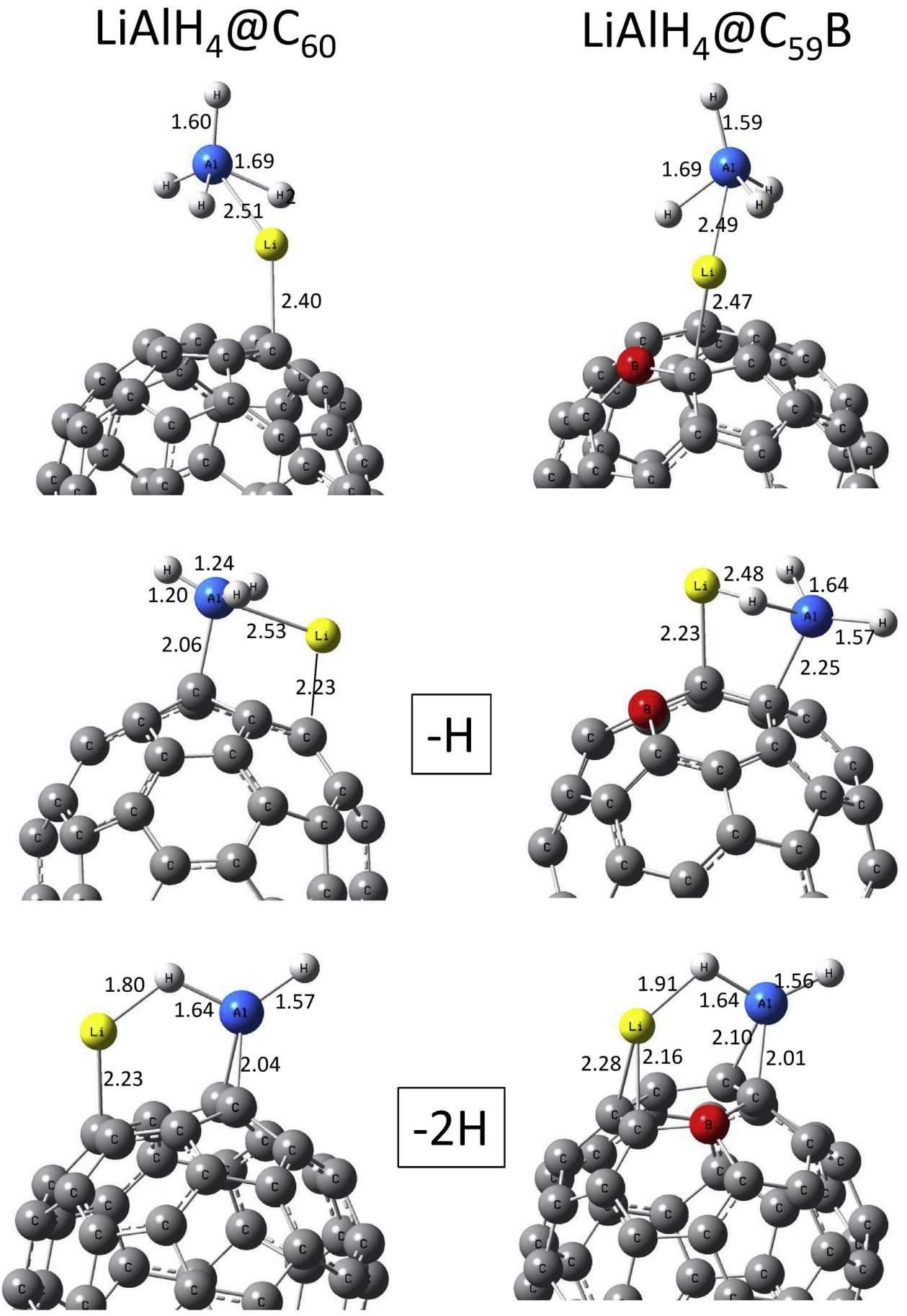

Fig. 3 – Optimized geometries for $LiAlH_4$ supported on C_{60} and C_{59} B as H atoms are removed.

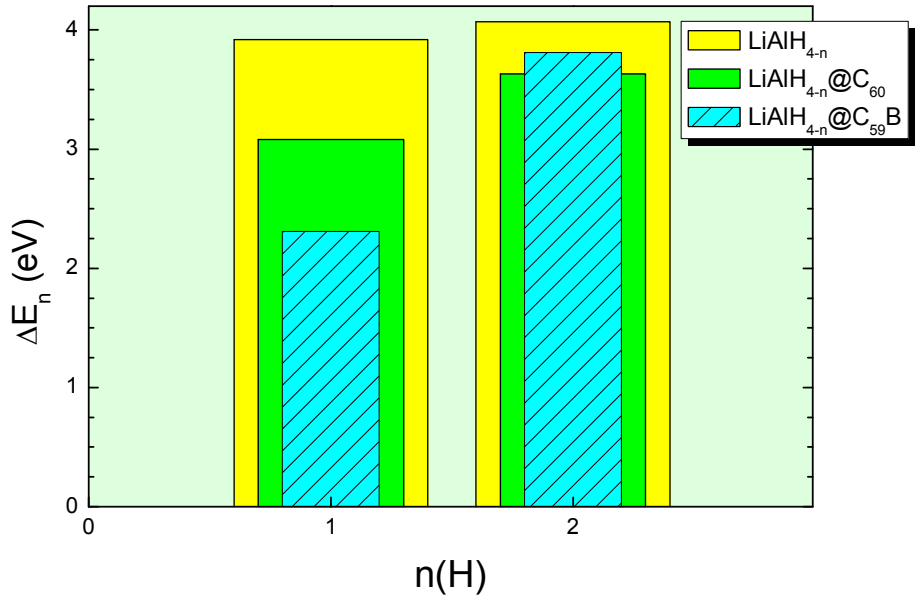

Fig. 4 – Energy cost Δ E (eV) for H-removal from $LiAlH_4$, $LiAlH_4@C_{60}$ and $LiAlH_4@C_{59}B$.

and C_{59} B fullerenes as catalysts are thus 25% and 31%, respectively.

The equilibrium geometries of the alanate clusters supported on C_{60} are showed in Fig. 3. Note that the $LiAlH_4$ cluster assumes a similar configuration in the presence of the fullerene as compared to the borane. We can see that upon the addition of the catalyst, the integrity of the $LiAlH_4$ cluster is still preserved; the Li–C bond length is 2.40 Å. After removing one H atom from the ligand radical of the $LiAlH_3$ we see some resemblance with the orientation assumed by the borane cluster, i.e., it stands also in a sideway configuration. The Li–C and Al–C bond lengths are 2.23 and 2.06 Å, respectively. Note how the remaining H atoms get closer to the Al atom. By removing another H atom we see almost the disruption of the alanate, which now is tightly bonded to the surface of the fullerene. On the right panels in Fig. 3 we can see the remarkable effect on this reaction of the boron doping the buckyball. Initially the Al–Li bond length is slightly shorter (2.49 Å), near the catalyst. The Li atom stay farther away from the fullerene too. With the first H removal the $LiAlH_3$ binds to the surface of the fullerene, showing longer Al–C bond length (2.25 Å) as compared to the pristine fullerene, whereas keeping practically same Li–C and Li–Al bond lengths. After removing two H atoms the cluster tends to disrupt, and both Li and Al atoms get more strongly bonded to the C atoms. Nevertheless, despite the slight distortion of the buckyball as the Li–Al cluster binds to it, we can see that the integrity of its shape is still sustained. The calculated energy cost for removing one and two H atoms from the $LiAlH_4$ cluster are 3.92 and 4.07 eV, respectively, as depicted in the histogram plots of Fig. 4. In the presence of the C_{60} this decreases to 3.08 and 3.63 eV, respectively, which represents a gain of about 21% for the first H removal. When using the B-doped C_{59} B fullerene the equivalent change in Δ E are 2.31 and 3.80 eV, respectively, which equals to a remarkable gain of about 41% for the first H removal from the $LiAlH_4$ cluster.

A Löwdin population analysis was performed in order to determine partial atomic charges in these clusters. For $LiBH_4@C_{60}$, the valence charge assigned to the Li, B and H atoms are 2.54, 3.56 and 0.99 e (on average), respectively, which implies a net charge of +0.46, −0.56 and +0.01 e, respectively. Boron is an acceptor while Li is a donor for electrons. The B–H bonds are of covalent nature, whereas the Li–B bonding is primarily ionic. With the removal of one and two H atoms, the charge on the Li atom remains at about 2.43 e, whereas on the B atom it decreases to 3.33 and 3.16 e, respectively, and the average charge on the H atoms decreases slightly to 0.98 to 0.97 e, respectively. In this way, by using the boron-doped fullerene in this reaction the partial charges on the Li atom changes from 2.44 to 2.42 and 2.47 e, whereas on the B this changes from 3.34 to 3.18 and 3.11 e, respectively, for the first and second H removal. The average charge on the H atoms now changes from 0.95 to 0.92 and 0.98 e, respectively. For $LiAlH_4@C_{60}$, the partial charge on the Li, Al and H atoms are 2.63, 2.44 and (average) 1.24 e, respectively. Both Al and Li are acceptors. By removing one and two H atoms the charge on the Li atom changes to 2.50 and 2.49 e, while on the Al atom it decreases to 2.27 and 2.13 e, and on the H atoms it changes

Table 1 – Calculated binding energy E_b and charge transfer Q of $LiBH_4$ and $LiAlH_4$ clusters supported on the pristine and B-doped C_{60} fullerene inasmuch as n(H) hydrogen atoms are removed.

n(H)	$LiBH_4@C_{60}$	$LiBH_4@C_{59}B$	$LiAlH_4@C_{60}$	$LiAlH_4@C_{59}B$
E_b (eV)				
0	0.39	0.31	0.57	0.05
1	1.20	1.66	0.33	1.56
2	2.84	2.58	1.86	1.83
Q (e)				
0	−0.05	0.42	0.00	0.00
1	0.30	0.64	0.52	0.56
2	0.43	0.45	0.93	0.57

to 1.23 and 1.25 e (on average), respectively. For the boron-doped system these are: Li (2.64, 2.56 and 2.84 e), Al (2.45, 2.25 and 2.54 e), H (average 1.23, 1.21 and 1.23 e), respectively.

The binding energy of the $LiBH_4$ cluster to C_{60} is calculated as

$$E_b = E[Li(BH_4)@C_{60}] - E[LiBH_4] - E[C_{60}]$$

which is a measure of the stability of the cluster. In this case $E_b = 0.39$ eV, indicating weak interaction. The calculated results are showed in Table 1. Upon the removal of one and two H atoms the binding energy increases to 1.20 and 2.84 eV, respectively. When using the boron-doped fullerene, $E_b = 0.31$ eV for the $LiBH_4@C_{60}$ system, and by removing one and two H atoms E_b increases significantly to 1.66 and 2.58 eV, respectively, revealing therein much stronger interaction. For the alanate cluster the calculated result for the binding energy is 0.57 eV, and upon the successive first and second H removals E_b changes to 0.33 and 1.86 eV, respectively. For the $LiAlH_4@C_{59}$ B system, the calculated binding energy is 0.05 eV, 1.56 and 1.83 eV, when considering 0, 1 and 2 H removals, respectively. These results therefore show a much weaker interaction between the alanate cluster and the fullerene, which becomes even more weaker upon boron-doping, and provide a reasoning for understanding the observed increase in the energy cost after the first H removal as being due to the onset of stronger interactions cluster-fullerene.

Let us now discuss the charge transfer mechanism: the calculated electron affinity of $LiBH_4$ and $LiAlH_4$ are 2.35 and 2.52 eV, whereas for C_{60} and C_{59} B it is 2.80 and 3.34 eV, respectively. Laser photo-detachment measurements on the C_{60} anion cooled in a storage ring yield an electron affinity value of 2.666 ± f 0.001 eV [32]. Notwithstanding its lower electron affinity, when $LiBH_4$ is supported on C_{60} it gets a small net influx of charge (−0.05 e) from the fullerene, which goes primarily to the B atom. The interaction between Li^+ and BH^-4 is therefore of ionic nature, whereas the Li–C bond has covalent nature. As it can be seen in Table 1, with the removal of one and two H atoms from $LiBH_4@C_{60}$ there is a loss of charge (Q) of 0.30 and 0.43 e from the cluster to the fullerene, whereas in the $LiBH_4@C_{59}$ B system, this corresponds to 0.64 and 0.45 e, respectively. Note in Table 1 that Q = 0 for both $LiAlH_4@C_{60}$ and $LiAlH_4@C_{59}$ B systems, and how there occurs a significant outflow of charge upon the H removal. In Fig. 5 is showed a diagram of the electronic energy levels (the Fermi level is shifted to the origin). Note the evolution of the gap between the valence states and the virtual (empty) bound states, and how the valence band edge is shifted upwards to higher energies in this reaction. Besides, with the hybridization which

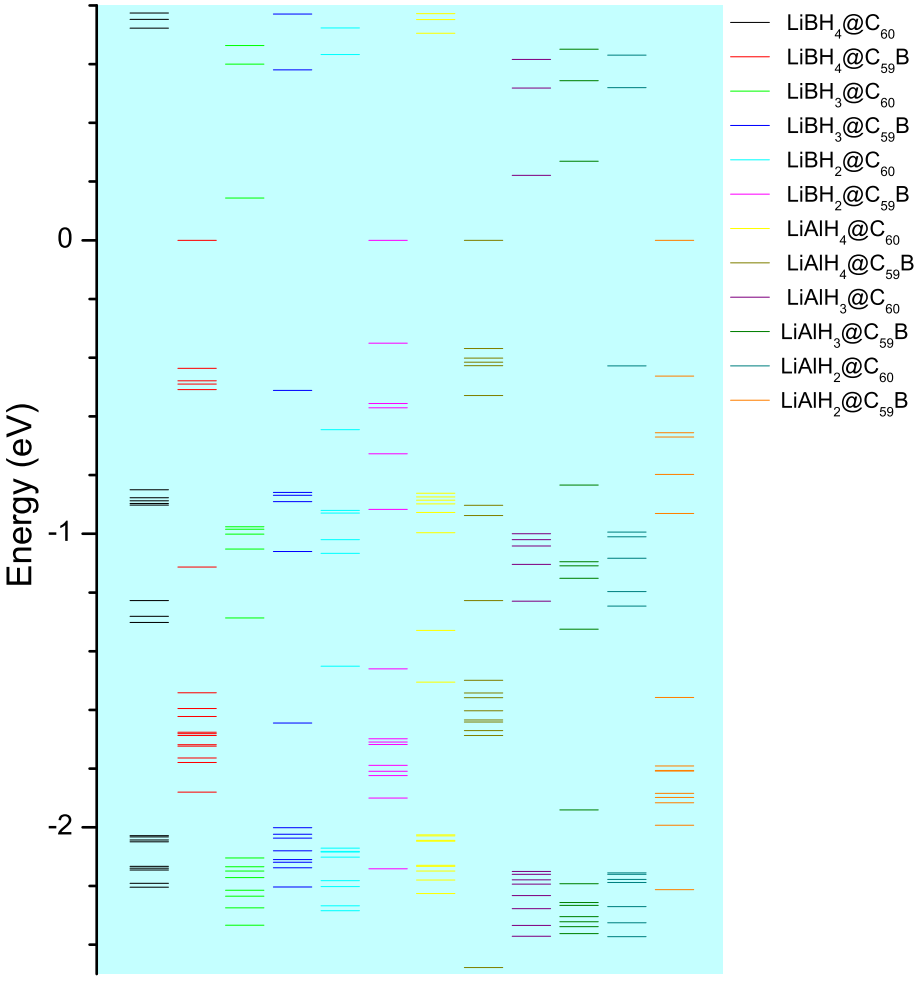

Fig. 5 – Electronic energy levels of $LiBH_4$ and $LiAlH_4$ clusters supported on C_{60} and C_{59} B fullerenes as H atoms are removed. The Fermi level is shifted to the origin.

takes place upon the binding of the cluster to the surface of the fullerene we can see the lifting of the degeneracy for the valence states. The loss of coupling upon the B-doping is clearly depicted in this diagram, as it can be seen with the increase in the energy of the bonding states. It is intriguing that the electron affinity does not play a major role. The cluster donates charge to the catalyst, an effect even more pronounced upon the B-doping. This reflects the stronger interaction which arises from the enhancement in the hybridization of the p-states which takes place in this reaction which in turn eases the transfer of electrons in the interplay between their hydride cluster and fullerene. It is worth to mention that alanates usually are less stables than the boranes, a feature which is also evidenced by the present calculations. Finally, this study shows that the performance of carbon fullerenes as catalysts for the dehydrogenation of the light metal hydrides $LiBH_4$ and $LiAlH_4$ is manifestly evident, and the boron-doping introduces a significant gain in the energy cost for this reaction to occur.

Conclusions

Summing up, first-principles calculations based on density functional theory are performed with the Quantum Espresso code to study the mechanism of hydrogen desorption from light metal hydrides by using the buckminsterfullerene C_{60} as catalyzing agent. In the presence of the catalyst the changes in the energy of the electronic states favor the onset of a weaker cohesion in the combined system, which in turn eases the H removal. Upon boron-doping the fullerene, besides keeping the integrity of its shape as well as of the hydride cluster, also contributes to establish a favorable mechanism of charge transfer and redistribution of bonding charge in the interplay between the alkali metal cluster and fullerene, and therein to weaken the interactions within the ligand complex which eases the hydrogen desorption. The present results show unequivocally a substantial decrease in the energy cost for hydrogen desorption after the addition of the nanostructured carbon catalyst, an effect which is particularly even more pronounced upon boron-doping. After binding to the fullerene the dehydrogenation process is favored as a result of enhanced instability of the hydride clusters driven by a shift of the hybridized electronic states towards higher energies at the molecular level.

Acknowledgments

This research was supported by grants from the Conselho Nacional de Desenvolvimento Cientiifico e Tecnológico (CNPq), Brazil. Computational support from the Centro Nacional de Processamento de Alto Desempenho da Universidade Federal do Ceará (CENAPAD-UFC) and Centro Nacional de Supercomputação da Universidade Federal do Rio Grande do Sul (CESUP), Brazil) are gratefully acknowledged. A.M.R. acknowledges support from the U.S. Department of Energy, Office of Basic Energy Sciences, under grant DE-FG02-07ER46431.

REFERENCES

[1] Galushkin NE, Yazvinskaya NN, Galushkin DN. Thermal runaway as a new high-performance method of desorption of hydrogen from hydrides. Int J Hydrogen Energy 2016;41:14813–9.
[2] Drozdov IV, Kochubey V, Meng Li, Mauer G, Vaßen R, Stöver D. Modelling and proper evaluation of volumetric kinetics of hydrogen desorption by metal hydrides. Int J Hydrogen Energy 2015;40:10111–22.
[3] Rusman NAA, Dahari M. A review on the current progress of metal hydrides material for solid-state hydrogen storage applications. Int J Hydrogen Energy 2016;41:12108–26.
[4] Chabane D, Harel F, Djerdir A, Candusso D, ElKedim O, Feninechе N. A new method for the characterization of hydrides hydrogen tanks dedicated to automotive applications. Int J Hydrogen Energy 2016;41:11682–91.
[5] Wu Z, Yang F, Zhu L, Feng P, Zhang Z, Wang Y. Improvement in hydrogen desorption performances of magnesium based metal hydride reactor by incorporating helical coil heat exchanger. Int J Hydrogen Energy 2016;41:16108–21.
[6] Bhihi M, Khatabi ME, Lakhal M, Naji S, Labrim H, Benyoussef S, et al. First principle study of hydrogen storage in doubly substituted Mg based hydrides. Int J Hydrogen Energy 2015;40:8356–61.
[7] Horikoshi S, Kamata M, Sumi T, Serpone N. Selective heating of Pd/AC catalyst in heterogeneous systems for the microwave-assisted continuous hydrogen evolution from organic hydrides: temperature distribution in the fixed-bed reactor. Int J Hydrogen Energy 2016;41:12029–37.
[8] Bürger I, Bhouri M, Linder M. Considerations on the H_2 desorption process for a combination reactor based on metal and complex hydrides. Int J Hydrogen Energy 2015;40:7072–82.
[9] Ahluwalia RK, Peng J-K, Hua TQ. Bounding material properties for automotive storage of hydrogen in metal hydrides for low-temperature fuel cells. Int J Hydrogen Energy 2014;39:14874–86.
[10] Bürger I, Luetto C, Linder M. Advanced reactor concept for complex hydrides: hydrogen desorption at fuel cell relevant boundary conditions. Int J Hydrogen Energy 2014;39:7346–55.
[11] Paidar V. Magnesium hydrides and their phase transitions. Int J Hydrogen Energy 2016;41:9769–73.
[12] Talagañis BA, Meyer GO, Aguirre PA. Modeling and simulation of absorption–desorption cyclic processes for hydrogen storage-compression using metal hydrides. Int J Hydrogen Energy 2011;36:13621–31.
[13] Schlapbach L, Züttel A. Hydrogen-storage materials for mobile applications. Nature 2001;414:353–8.
[14] Crabtree W, Dresselhaus MS, Buchanan MV. The hydrogen economy. Phys Today 2004;57:39–44.
[15] Grochala W, Edwards PP. Thermal decomposition of the non-interstitial hydrides for the storage and production of hydrogen. Chem Rev 2004;104:1283–315.
[16] Orimo S, Nakamori Y, Kitahara G, Miwa K, Ohba N, Towata S, et al. Dehydriding and rehydriding reactions of LiBH4. J Alloys Compd 2005;427:404–6.
[17] Bogdanović B, Schwickardi M. Ti-doped alkali metal aluminium hydrides as potential novel reversible hydrogen storage materials. J alloys and Compd 1997;20:1–9.
[18] Bogdanović B, Felderhoff M, Kaskel S, Pommerin A, Schlichte K, Schüth F. Improved hydrogen storage properties of Ti-doped sodium alanate using titanium nanoparticles as doping agents. Adv Mater 2003;15:1012–5.
[19] Luo W, Gross KJ. A kinetics model of hydrogen absorption and desorption in Ti-doped NaAlH4. J Alloys Compd 2004;385:224–31.

[20] Araújo CM, Li S, Ahuja R, Jena P. Vacancy-mediated hydrogen desorption in NaAlH4. Phys Rev B 2005;72:165101.
[21] LOM, Opalka SM. Density functional calculations of Ti-enhanced NaAlH4. Phys Rev B 2005:71. 054103.
[22] Paduani C. A study of the effect of the addition of nanostructured carbonaceous catalysts in the dehydrogenation mechanism of magnesium borohydride. J Mater Chem A 2015;3:819–24.
[23] Stowe A, Teprovich Jr JA, Knight DA, Wellons MS, Zidan R. Catalytic Carbon Nanostructures and Novel Nanocomposites for Hydrogen Storage. J S C Acad Sci 2011;9:13.
[24] Scheicher RH, Li S, Araújo CM, Blomqvist A, Ahuja R, Jena P. Theoretical study of C60 as catalyst for dehydrogenation in LiBH4. Nanotechnology 2011:22. art. no. 335401.
[25] Wellons MS, Berseth PA, Zidan R. Novel catalytic effects of fullerene for LiBH4 hydrogen uptake and release. Nanotechnology 2009;20:204022.
[26] Guo T, Jin C, Smalley RE. Doping bucky: formation and properties of boron-doped Buckyminsterfullerene. J Phys Chem 1991;95:4948–50.
[27] Giannozzi P, Baroni S, Bonini N, Calandra M, Car R, Cavazzoni C, et al. QUANTUM ESPRESSO: a modular and open-source software project for quantum simulations of materials. J Phys: Condens. Matter 2009;395502:21. URL http://www.quantum-espresso.org.
[28] Thonhauser T, Zuluaga S, Arter CA, Berland K, Schrder E, Hyldgaard P. Spin signature of nonlocal correlation binding in metal-organic frameworks. PRL 2015;115:136402. ; Thonhauser T, Cooper VR, Li S, Puzder A, Hyldgaard P, Langreth DC. Van derWaals density functional: self-consistent potential and the nature of the van der Waals bond Phys Rev B 2007;76:125112.
[29] Berland K, Cooper VR, Lee K, Lundqvist BI. Van der Waals forces in density functional theory: a review of the vdW-DF method. Rep. Prog. Phys 2015:78. 066501.
[30] Langreth DC, Lundqvist BI, Chakarova-Käck SD, Cooper VR, Dion M, Hyldgaard P, et al. A density functional for sparse matter. J Phys Condens Matter 2009:21. 084203.
[31] Grimme S. Semiempirical GGA-type density functional constructed with a long-range dispersion correction. J Comp Chem 2006;27:1787.
[32] Brink C, Andersen LH, Hvelplund P, Mathur D, Voldstad JD. Laser photodetachment of C60 and C70 ions cooled in a storage ring. Chem Phys Lett 1995;233:52.